OUKA
The University of Osaka
Institutional Knowledge Archive

Title	Effect of Oxygen Content in He-O_2 Shielding Gas on Weld Shape in Ultra Deep Penetration TIG
Author(s)	Fujii, Hidetoshi; Lu, Shanping; Sato, Toyoyuki et al.
Citation	Transactions of JWRI. 2008, 37(1), p. 19-26
Version Type	VoR
URL	https://doi.org/10.18910/6051
rights	
Note	

The University of Osaka Institutional Knowledge Archive : OUKA

https://ir.library.osaka-u.ac.jp/

The University of Osaka

Effect of Oxygen Content in He-O_2 Shielding Gas on Weld Shape for Ultra Deep Penetration TIG †

FUJII Hidetoshi*, LU Shanping **, SATO Toyoyuki* and NOGI Kiyoshi******

Abstract

A new type of TIG welding has been developed, in which an ultra-deep penetration (10mm for one pass) is obtained. In order to control the Marangoni convection induced by the surface tension gradient on the molten pool, He gas containing a small amount of oxidizing gas was used. The effect of the concentration of O_2 and CO_2 in the shielding gas on the weld shape was studied for the bead-on-plate TIG welding of SUS304 stainless under He-O_2 and He-CO_2 mixed shielding gases. Because oxygen is a surface active element for stainless steel, the addition of oxygen to the molten pool can control the Marangoni convection from the outward to inward direction on the liquid pool surface. When the oxygen content in the liquid pool is over a critical value, around 70ppm, the weld shape suddenly changes from a wide shallow shape to a deep narrow shape due to the change in the direction of the Marangoni convection. Also, for He based shielding gas, a high welding current will strengthen both the inward Marangoni convection on the pool surface and the inward electromagnetic convection in the liquid pool. Accordingly, at a welding speed of 0.75mm/s, the welding current of 160A and the electrode gap of 1mm under the He-0.4%O_2 shielding, the depth/width ratio reaches 1.8, which is much larger than for Ar-O_2 shielding gas (0.7) and Ar shielding gas (0.2). The effects of the welding parameters, such as welding speed and welding current, were also systematically investigated. In addition, a double shielding gas method has been developed to prevent any consumption of the tungsten electrode. along the heating line, the inherent deformation of smaller plates, with the same thickness and formed under the same heating and cooling conditions, can be accurately and easily predicted.

KEY WORDS: (Weld shape) (Oxygen) (Helium) (Marangoni convection) (Electromagnetic convection) (Double shielding gas) (Welding current) (Welding speed) (Tensile strength) (Charpy impact test) (Bending test)

1. Introduction

TIG welding is one of the most popular welding processes in various manufacturing industries due to the good weld bead surface obtained and a very high quality weld metal without any weld defects. However, compared to other arc welding processes, such as gas metal arc welding, plasma arc welding, or submerged arc welding, the shallow penetration of the TIG welding restricts its ability to weld thick structures in a single pass, thus its productivity is relatively low. Therefore, in order to increase the TIG welding production, the demand for control of the weld shape with a deep penetration is steadily increasing, and has been a concern for a long time.

Some experimental studies reported that the TIG weld shape in stainless steel and other materials varied with a change in the concentration of one or more impurities in the raw materials[1-6]. In order to increase the TIG welding production, the demand for the automatic and precise control of the weld shape with deep penetration is steadily increasing, and has been a concern for a long time. Recently, a novel modification of the TIG process, active flux TIG (A-TIG), which was first proposed by E.O.Paton Institute of Electric Welding in the 1960s[7], has been brought to many researchers' attention since 1980s. Even though some fluxes for the A-TIG process are commercially available and have been applied in industry, there is still no common agreement on the understanding of the A-TIG mechanism. There have been four physical mechanisms that are possible contributors to the A-TIG mechanism. The first is that a lowering of the surface tension of the molten pool by the flux results in an increased depression of the surface of the weld pool to provide an increased radius of curvature of the weld pool surface to support the arc pressure, and this is also called the TIG keyhole mode[8]. The second mechanism is the arc constriction produced by the vaporized flux molecules[9-16]. The third one is the reversal of the Marangoni convection, which is induced by the change in the sign of the temperature coefficient of the

† Received on July 11, 2008
* Associate Professor
** Specially Appointed Researcher,
*** Taiyo Nippon Sanso Corporation, Yamanashi 408-0015
**** Professor
Transactions of JWRI is published by Joining and Welding Research Institute, Osaka University, Ibaraki, Osaka 567-0047, Japan

surface tension when the surface active element is over a critical value in the liquid pool[5, 6, 17-21]. Recently, Lowke and co-workers proposed another mechanism call the insulation mode[22].

A better understanding of the A-TIG behavior is important in order to raise TIG welding productivity. The authors conducted stainless welding using various oxide fluxes as a surface active agent, and found that the reverse Marnagoni convection is induced. This behavior was considered to be a governing mechanism of A-TIG welding[19, 20]. They further investigated the effect of a small addition of active gas such as O_2 and CO_2, to the inert argon shielding gas, without using oxide flux, to eliminate the sensitive effect of oxides[21, 23, 24]. This finding makes it possible to develop an advanced automatic TIG welding process because the amount of oxygen in a weld pool can be more precisely controlled by adding active gas into shielding gas than by putting oxide flux on plates as is done in the conventional A-TIG process.

Helium is another important inert gas for TIG welding. Compared to argon, it has large thermal conductivity (Ar:53mW/mK; He: 460mW/mK), and the current density at the anode spot in the liquid pool under He shielding is high, which will directly increase the electromagnetic force and possibly increase the temperature gradient on the pool surface. Since the strength of the Marangoni convection is controlled by the combination of the temperature gradient on the pool surface and the temperature coefficient of surface tension, the helium arc should also have certain effect on the Marangoni convection. Under the cooperation of the strong electromagnetic convection in the liquid pool and the inward Marangoni convection on the pool surface, the TIG weld penetration is possibly improved significantly. In this study, TIG welding was conducted under various conditions using He shielding gas with small additions of O_2 or CO_2 in order to find the effect of mixed gas and welding conditions on the Marangoni convection as well as the shape of the weld pool.

2. Experimental

The TIG bead-on-plate welds were produced on SUS304 stainless steel plates (100×50×10mm), with the lower oxygen content, 38ppm, and sulfur content, 5ppm. The detailed chemical composition of the substrate is given in **Table 1**. Prior to welding, the surface of the plate was ground using an 80-grit flexible abrasive paper and then cleaned by acetone.

A direct current, electrode negative (DCEN) polarity power source (YC-300BZ1) was used with a mechanized system in which the test piece was moved at a constant speed. A water-cooled torch with a thoriated tungsten

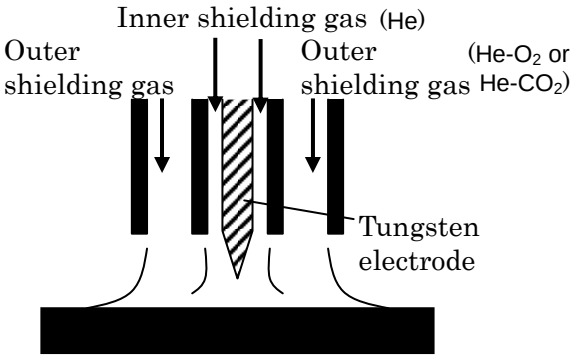

Fig.1 Schematic diagram of double shielding torch for TIG welding.

electrode (W-2%ThO_2, Φ2.4mm) was used in the experiments. The vertex angle of the electrode was 60^0 and the gas flow rate was set at 10L/Min for all experiments.

For the first step experiments, all the bead-on-plate welds were made under identical welding conditions with the welding current, 160A, welding speed, 2mm/s and the electrode gap, 3mm, except that the torch gas concentration was varied between pure helium and helium with 4%O_2. After that, the effect of welding parameters including welding current and welding speed on the weld shape was investigated under pure He and He-0.4%O_2 shielding, separately. The welding current varied from 80A to 250A, and the welding speed changed between 0.75mm/s to 5.0mm/s.

For the next step, a double shielding torch was used to decrease the consumption of the tungsten electrode. A schematic diagram of the double shielding torch is shown in **Fig.1**. The outer shielding gas was a He-O_2 or He-CO_2 mixed gas, and the inner shielding gas was pure He gas.

After welding, all the weld beads were sectioned and specimens for the weld shape observations were prepared by etching using a HCl + Cu_2SO_4 solution to reveal the bead shape and dimensions. The cross-sections of the weld bead were photographed using an optical microscope (Olympus HC300 Z/OL). The oxygen content in the weld metal was analyzed using an oxygen/nitrogen analyzer (Horiba, EMGA-520). Samples for the oxygen measurement were cut directly from the weld metal.

Some test plates (500mm×300mm×10mmt) were welded with I type butt joints by a one pass layer from both the face and the back side using the double shielding torch. The mechanical properties of the welded joints were evaluated using a tensile test, a bending test, and a V-notched Charpy impact test.

Table 1 Chemical composition of SUS304 stainless steel.

Element	C	Si	Mn	Ni	Cr	P	S	O	Fe
(wt%)	0.06	0.44	0.96	8.19	18.22	0.027	0.0005	0.0038	Bal.

3. Results

3.1 Weld shape and Marangoni convection

Representative weld cross-sections under different torch gas shielding from pure He to He-4%O_2 shielding are shown in **Fig.2** with the standard welding conditions of welding current of 160A, welding speed of 2mm/s and the electrode gap of 3mm. There was a distinct change in the weld shape profile under different torch gas compositions. Welds produced under pure He and He-0.1%O_2 shielding are relatively wide shallow as shown in Figs.2a and b. When the oxygen content in the shielding gas is in the range of 0.2% to 2.0%, the weld shape become relatively narrow and deep as shown in Figs.2c to h. With further increasing the oxygen content in the shielding gas, it is interesting to find that the weld shape become shallow and wide again as shown in Figs. 2i and j.

Figure 3 shows the effect of torch gas oxygen content on the weld depth/ width (D/W) ratio and the weld metal oxygen content. The weld D/W ratio is lower around 0.4 under pure He shielding and He-0.1%O_2 mixed shielding, and abruptly increases and reaches to 0.6 when the oxygen concentration in the shielding gas is between 0.2% to 2.0%. This sharply increasing of the D/W ratio indicates that the fluid flow pattern in the liquid pool is possibly changed. When the torch gas oxygen concentration is over 2%, the weld D/W ratio decreases again. The weld metal oxygen content continuously increases with an increase in the torch gas oxygen content, so that the weld metal oxygen content can be precisely controlled by the small addition of oxygen gas into the helium shielding gas.

The final weld shape of TIG welding on SUS304 stainless steel depends to a large extent on the different fluid flow modes in the welding pool, which was driven by the combination of the electromagnetic force, surface tension, buoyancy force and impinging force of the arc plasma, and the Marangoni convection induced by surface tension on the pool surface is the main convection that significantly influences the fluid flow in the liquid pool[6, 25-27]. Generally, the surface tension decreases with increasing temperature, $d\sigma/dT<0$, for a pure metal and many alloys. Since there is a large temperature gradient existing on the weld pool surface between the center under the torch and the edges of the weld pool, a large surface tension gradient will be produced along the surface. In the weld pool for such materials, the surface tension is higher in the cooler part of the pool, at the edge, than in the pool center, under the arc, and hence, the Marangoni convection flows from the pool center to the edge. The heat flux from the arc power in the pool center is easily transferred to the edge and the weld shape is relatively wide and shallow as shown in **Fig.4(a)**.

Sahoo et al.[26] studied the surface tension of binary

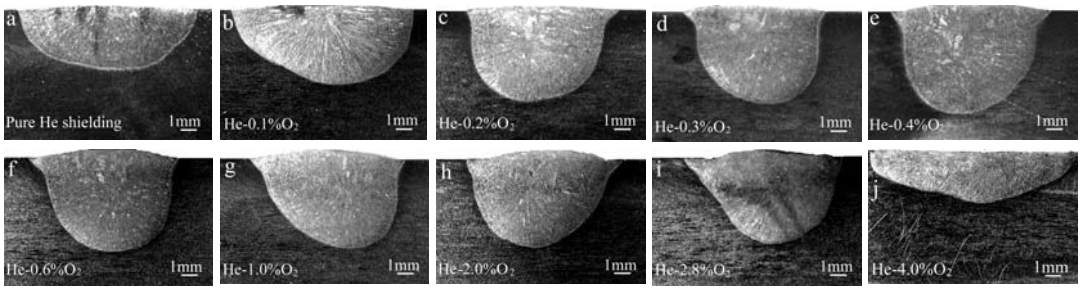

Fig.2 Weld shapes under different He-O_2 mixed shielding gases. (160A, 2mm/s, 3mm arc length)

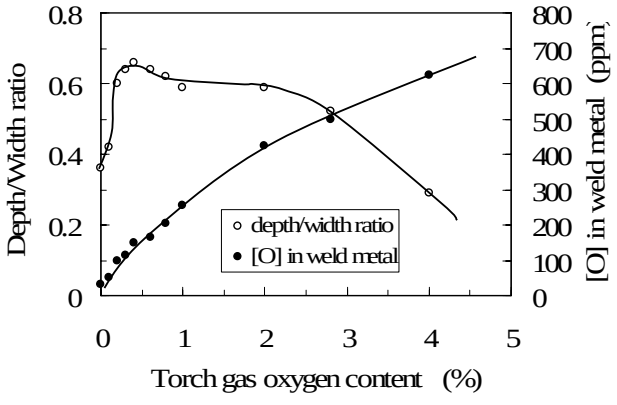

Fig.3 Effect of shielding gas oxygen content on the weld depth/width ratio and weld metal oxygen content. (160A, 2mm/s, 3mm arc length)

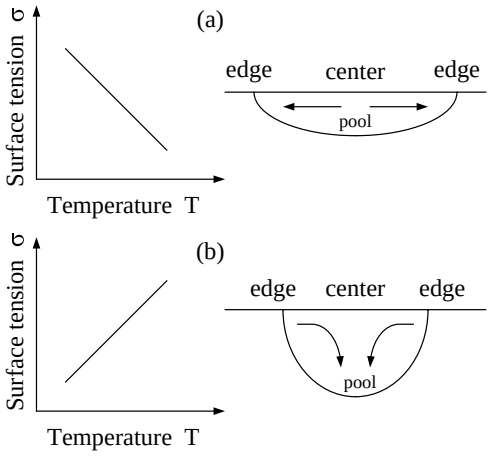

Fig.4 Marangoni convection mode in weld pool.
(a) $\partial\sigma/\partial T<0$; (b) $\partial\sigma/\partial T>0$

metals and calculated the temperature coefficient of the surface tension for the Fe-O and Fe-S system. They found that the temperature coefficient of the surface tension is always negative for a low oxygen content in iron (< 20 ppm). On the other hand, for higher oxygen contents, it can change from a positive value at relatively low temperatures to a negative value at higher temperatures. Taimatsu et al. [28] measured the surface tension of Fe-O system at high temperature and found that the temperature coefficient of surface tension can change from a negative value to positive when the oxygen content in the Fe-O system is in the range of 150ppm to 500ppm. Therefore, oxygen and sulfur are the surface active elements for iron base alloys. When the surface-active element exceeds a certain value in stainless steel[5, 6], the temperature coefficient of the surface tension ($d\sigma/dT$) changes from a negative to a positive value, $d\sigma/dT > 0$, and the direction of the Marangoni convection on the weld pool changes as illustrated in **Fig. 4(b)**. In this case, the heat flux easily transfers from the center to the bottom and a relatively deep and narrow weld is made. Earlier experiments results[19, 20] showed that the oxygen was an active element in SUS304 stainless steel and the

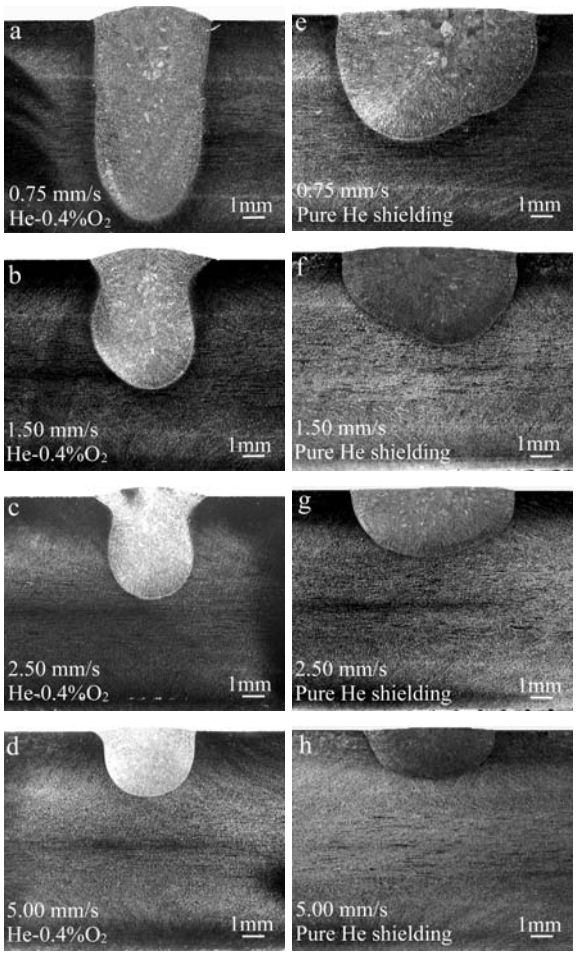

Fig.5 Weld shape at different welding speeds for pure He and He-0.4%O_2 shielding gases.

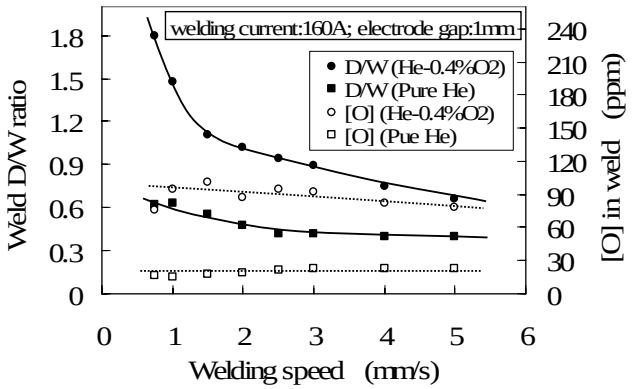

Fig.6 Effect of welding speed on weld depth/width ratio and weld metal oxygen content.

temperature coefficient of surface tension become positive when the oxygen content in the weld pool is in the range of 70ppm to 300ppm.

Addition of oxygen to the helium base shielding gas makes the oxygen content increase with the torch gas oxygen content as shown in Fig.3. When the oxygen concentration in the shielding gas reaches 0.2%, the weld metal oxygen content is 99.7ppm, which is over the critical value for positive temperature coefficient of surface tension and makes the outward Marangoni convection change to inward direction. Therefore, the weld shape changes from relative wide and shallow shape (Figs.2a and b) to narrow and deep shape (Figs.2c to h), and the weld depth/width ratio suddenly increases from 0.4 to 0.6 as shown in Fig.3. When the oxygen concentration in the shielding gas is over 2.0%, the weld metal oxygen content is over 400ppm as shown in Fig.3. In this case, the Marangoni convection on the liquid pool surface possibly changes to outward again, and makes weld depth/width ratio decrease as shown in Fig.3. The weld shape becomes relatively wide and shallow as shown in Figs.2i and j.

3.2 Effect of welding current on weld shape

Weld shape variations under different welding parameters including weld current, speed and electrode gap were systematically investigated under pure He and He-0.4%O_2 mixed shielding. **Figure 5** shows the weld shapes with different welding speed from 0.75mm/s to 5.0mm/s at constant welding current of 160A and electrode gap of 1mm. All the weld shapes are narrow and deep under He-0.4%O_2 mixed shielding as shown in Figs.5a to d, and wide and shallow weld shapes form under pure He shielding in Figs.5e to h. When the welding speed is at 0.75mm/s under He-0.4%O_2 shielding, a 10 mm weld penetration is obtained in single pass welding. **Figure 6** shows the weld metal oxygen content and weld depth/width ratio (D/W ratio) at different welding speeds under pure He and He-0.4%O_2 shielding gases. Under pure He shielding, the weld metal oxygen

content is around 20ppm, which is lower than (70-100) ppm under He-0.4%O_2 mixed shielding. Therefore, an outward Marangoni convection under pure He shielding and inward Marangoni convection under He-0.4%O_2 occurs on the liquid pool surface, which makes the weld shape deep and narrow under He-0.4%O_2 shielding as shown in Figs.5a to d, and wide and shallow as shown in Figs.5e to h under pure He shielding. The weld D/W ratio under He-0.4%O_2 shielding decreases with the increasing welding speed, and it is not sensitive to the welding speed under Pure He shielding.

The TIG weld shape on stainless steel depends to a large extent on the direction and magnitude of the Marangoni convection, which is determined by the product of the temperature coefficient of the surface tension ($d\sigma/dT$) and the temperature gradient (dT/dr) on the pool surface. Therefore, all factors that affect the temperature coefficient of the surface tension or the temperature distribution on the pool surface control the Marangoni convection in the liquid pool. The sign of $d\sigma/dT$ determines the Marangoni convection direction on the pool surface. The values of $d\sigma/dT$ and dT/dr determine the strength of the Marangoni convection. In TIG welding, the peak temperature and temperature gradient on the pool surface are affected by the heat input distribution. A distributed heat source conduction model by Burgardt[29] showed that lower welding speed will increase the temperature gradient and the peak temperature on pool surface. This was also was experimentally recognized by Sundell[30]. Therefore, it is proposed here that increasing the welding speed will decrease the peak temperature and the temperature gradient on the pool surface. A lower temperature gradient weakens the strength of the Marangoni convection on the pool surface. In the case where the inward Marangoni convection occurs under the He-0.4%O_2 shielding gas, the weaker the inward Marangoni convection under high welding speed, the lower is the weld D/W ratio as shown in Fig.6. However, for the outward Marangoni convection pattern under pure He shielding gas, the weak outward Marangoni convection leads to a decreasing the weld width with the increasing welding speed, which will impede the decrease in the surface temperature gradient and therefore the weld D/W ratio is not sensitive to the welding speed under pure He shielding as shown in Fig.6. These results are in good agreement with the findings by Burgardt and Heiple[29], and Shirali and Mills[31] about the effect of the welding speed on the weld shape for stainless steel with different sulfur contents.

3.3 Effect of welding current on weld shape

Figure 7 shows the effect of welding current on the weld shape under He-0.4%O_2 and pure He shielding at a constant welding speed of 2mm/s and electrode gap of 1mm. The weld shape is narrow and deep as shown in Figs.7(a to d) under He-0.4%O_2 shielding, and a relatively wide and shallow weld shape obtains under pure He shielding as shown in Figs.7(e to h). **Figure 8** gives the weld depth/width ratio and weld metal oxygen content at different welding currents. The weld metal oxygen content under pure He shielding is around 20ppm and an outward Marangoni convection occurs, which make the weld shape wide and shallow. Under He-0.4%O_2 shielding gas, the weld metal oxygen content is high between 70ppm to 110ppm and an inward Marangoni convection occurs on the liquid pool, thus a deep and narrow weld shape forms as shown in Figs.7(a to d). Under pure He shielding, the weld D/W ratio weakly decreases with the increasing welding current.

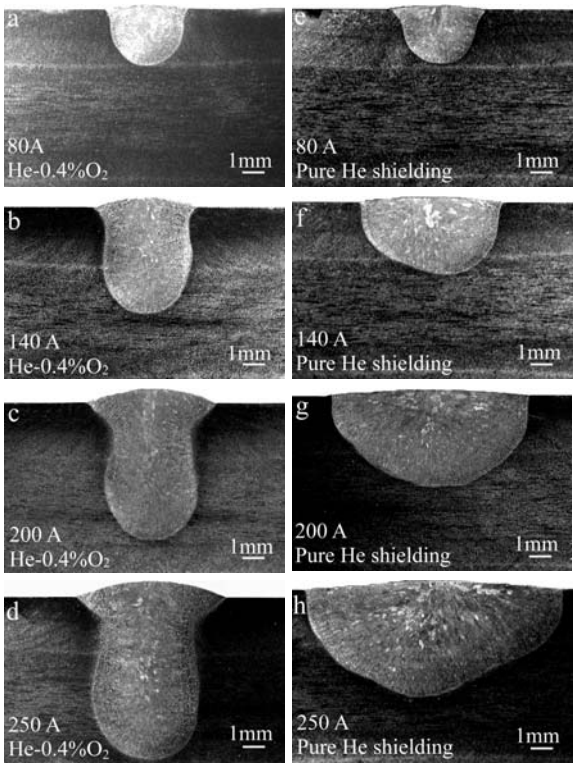

Fig.7 Weld shapes at different welding current for pure He and He-0.4%O_2 shielding gases.

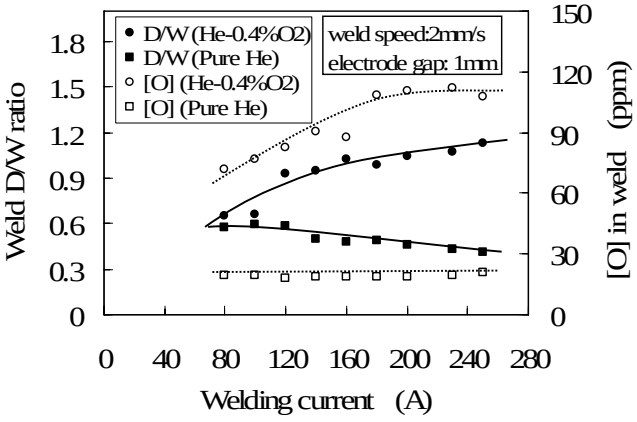

Fig.8 Effect of welding current on weld depth/width ratio and weld metal oxygen content.

However, under He-0.4%O_2 mixed shielding gas, the weld D/W ratio continuously increases with the welding current, which is quite different from the results under Ar-0.3%O_2 and Ar-0.3%CO_2 mixed shielding gases[24, 32], where the weld D/W ratio weakly decreases or keeps a constant value at high welding current.

Changing the welding current will directly alter the heat input and weld area. The heat distribution of the arc on the weld pool is the main factor affecting the weld shape and weld D/W ratio. Tsai and Eagar[33] observed that increasing the welding current would increase the magnitude of the heat intensity and widen the heat distribution of the arc on the pool surface. However, the heat distribution width weakly increases compared with the magnitude of the heat density. The higher the magnitude of the heat density, the larger is the temperature gradient on the pool surface. Therefore, the Marangoni convection on the pool surface should be strengthened with increasing welding current. Also, the large welding current should increase the strength of the electromagnetic convection in the liquid pool. The numerical study by Tanaka and Ushio[34] for the TIG welding indicated that the convection flow in the liquid pool was mainly controlled by the Marangoni force and electromagnetic force under pure He shielding. Under argon shielding, the plasma drag force and Marangoni force are the main forces controlling the liquid pool convection. Under He-0.4%O_2 mixed shielding, the large welding current will directly strengthen the inward Marangoni convection on pool surface and the inward electromagnetic convection in the liquid pool, which cause the weld D/W ratio continuously increase with welding current as shown in Fig.8. However, under Ar-0.3%O_2 and Ar-0.3%CO_2 shielding gases [24, 32], the plasma drag force that induces outward convection in the liquid pool is one of the main causes of convection, and large welding current will increase the plasma drag force, and thus make the weld D/W ratio weakly decrease or keep a constant value at high welding current under Ar-0.3%O_2 or Ar-0.3%CO_2 shielding gases.

Under pure He shielding gas, the Marangoni convection in the liquid pool is in outward direction. Large welding current will strengthen the outward Marangoni convection on the pool surface, will also strengthen the inward electromagnetic convection in the liquid pool. Under the combination of the two convections, the weld D/W ratio under pure He shielding is not sensitive to the welding current as shown in Fig.8. The slightly decreasing in the weld D/W ratio with increasing welding current also indicates that the effect of the Marangoni convection is stronger than that of electromagnetic convection.

3.4 Effect of double shielding torch

A double shielding gas method has been developed to prevent any consumption of the tungsten electrode. **Figure 9** shows the surfaces of the tungsten electrode after welding using the different shielding torches and shielding gases. In this case, the inner gas was pure He and the outer gas was He-CO_2 gas. For the normal torch,

Shielding gas	Normal single torch	Double Shielding torch
He-0.2%CO_2		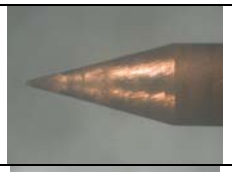
He-0.5%CO_2		
He-1.0%CO_2		
He-5.0%CO_2		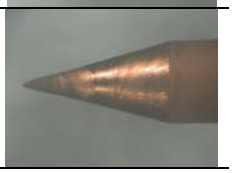

Fig.9 Surfaces of tungsten electrodes after welding by using different shielding torches and shielding gases.

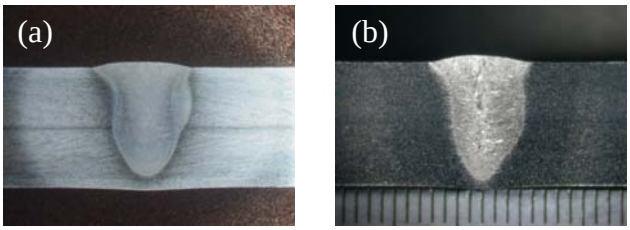

Fig.10 Comparison of weld shapes between (a)He-O_2 and (b)HeCO_2 as outer shield in double shielded TIG welding.

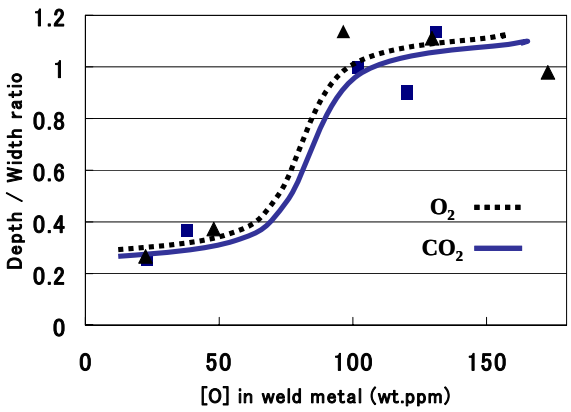

Fig.11 Relationship between oxygen content in weld pool and D/W ratio.

Table 2 Tensile strength of butt joints welded by double shielded TIG welding.

Test specimen No.	Tensile strength (N/mm2)	Broken Position
T1	593	Weld metal
T2	588	Weld metal

Table 3 Impact test result of butt joints welded by double shielded TIG welding.

Spec. No.	Position of V-notch	Absorbed energy (J)		Ratio of ductile fracture area (%)		Lateral Expansion (mm)	
			Ave.		Ave.		Ave.
CD1	Weld metal	82	85	100	100	1.37	1.41
CD2		83		100		1.38	
CD3		89		100		1.49	
CD4	Heat affected zone	177	176	100	100	2.17	2.23
CD5		173		100		2.20	
CD6		179		100		2.33	

a remarkable consumption of the tungsten electrode is clearly observed. On the other hand, for the double shielding torch, there is no consumption of any tungsten electrode even though a substantial amount of oxidizing gas was added.

Figure 10 shows the effect of the outer shielding gas on the cross-sections of the welds. The inner gas was pure He for both cases and the outer shielding gas was the He-O_2 or He-CO_2 gas. The welding speed, welding current and arc length were 120A, 1mm/min and 3mm, respectively. **Figure 11** shows that the relationship between the oxygen [O] content in the welds and the ratio of the depth to width (D/W). It was found that there is no difference in the penetration between the He-O_2 gas and He-CO_2 gas. When the oxygen [O] content of the welds is over 70ppm, the D/W of the welds sharply increases regardless of the oxidizing gas such as O_2 or CO_2, which is completely same as the case for the normal torch.

3.5. Evaluation of the Quality of welded joints

Table 2 shows the result of the tensile tests for the joints welded under the conditions shown in section 3.4 using the double shielding gas torch. The tensile strength of the joints is much stronger than the value of the base metal standard (520N/mm^2: JIS G 4304).

Table 3 shows the result of the V-notch Charpy impact test. The test specimens are sub-sized with a three-quarter thickness (t7.5mm), and the test temperature is –196° (liquid nitrogen). Both the absorbed energy values of the weld metal and the heat affected zone are sufficient for the TIG welded joint, and the ratio of the ductile fracture area and the lateral expansion also show the high toughness characteristics of this joint.

Figure 12 shows the bending test results and a photograph of the test specimens after the bending test.

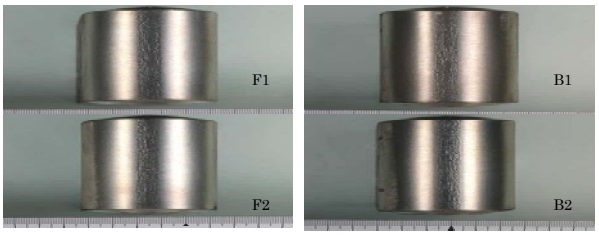

(a)Face side (b) back side

Fig.12 Photographs of bending test specimens.

The test specimens were bent up to 180°using a guide whose bending radius was twice that of the specimen thickness. There was no defect on either side of all the specimens. These results clearly showed the soundness of the welded joints. Based on these three kinds of mechanical tests, it can be judged that the quality of the welded joints is as good as the normal TIG welding joints, even if these joints are welded using a slightly oxidizing gas as the outer shielding gas.

Therefore, this new double shielded TIG welding process is definitely applicable for many industrial welding processes. In this case, the usual welding equipment can be used.

4. Conclusions

(1) When the oxygen concentration in the He based shielding is in the range of 0.2% to 2.0%, the weld metal oxygen content is over the critical value of 70ppm, and an inward Marangoni convection occurs, which makes the weld shape become deep and narrow. When the oxygen content in the shielding gas is below 0.2% or over 2.0%, the inward Marangoni convection changes from inward to outward and the weld shape becomes shallow and wide.

(2) The TIG weld shape in stainless steel depends to a large extent on the pattern and strength of the Marangoni convection, which is controlled by the combinations of the weld metal oxygen content, as a surface active element, temperature coefficient of surface tension and the temperature gradient on the pool surface. Different welding parameters will change the temperature gradient on the pool surface, and ultimately change the strength of the Marangoni convection.

(3) At the lower welding speed of 0.75mm/s, the welding current of 160A and the electrode gap of 1mm under the He-0.4%O_2 shielding, the weld penetration reaches 10mm for a single pass weld, which is much deeper for Ar-O_2 shielding gas.

(4) For He based shielding gas, a high welding current will strengthen both the inward Marangoni convection on the pool surface and the inward electromagnetic convection in the liquid pool, which

make the weld depth/width ratio continuously increase with the welding current.

(5) By using the double shielding torch instead of the normal torch for the TIG welding, the degree of the consumption of the tungsten electrode can be the same as for normal TIG welding even when an oxidizing gas is included in the shielding gas.

(6) The joint welded by this new TIG process in which a slightly oxidizing gas is used as the outer gas in the double shielding torch has sound mechanical properties including the tensile Charpy and bending tests. Therefore, this new double shielded TIG welding process is definitely applicable for many industrial welding processes.

Acknowledgement

This study was supported by the New Energy and Industrial Technology Development Organization (NEDO) of Japan, the Global Century COE Program, ISIJ research promotion grant, and JFE 21st Century Foundation.

References

1) W.F.Savage, E.F.Nippes and G.M.Goodwin: Weld.J., 1977,vol.56, pp126s-132s.
2) G.W.Oyler, R.A.Matuszesk and C.R.Carr: Weld.J., 1967, vol.46, pp1006-1011.
3) W.S.Bennett and G.S.Mills: Weld.J., 1974, vol.53, pp548s-553s.
4) B.E.Paton: Automat.Weld., 1974, vol.27, pp1-4.
5) C.R.Heiple and J.R.Ropper: Weld.J., 1981, vol.60, pp143s-145s.
6) C.R.Heiple and J.R.Ropper: Weld.J., 1982, vol.61, pp97s-102s.
7) S.M.Gurevich and V.N.Zamkov: Avtom.Svarka., 1966, No.12, pp13-16.
8) M.M.Savitskii and G.I.Leskov: Avtom.Svarka., 1980, No.9, pp17-22.
9) P.J.Modenesi, E.R.Apolimario and I.M.Pereira, J of Mater.Proc.Tech., 2000, vol.99, pp260-265.
10) S.Kou and Y.H.Wang, Weld.J., 1986, vol.65, pp63s-70s.
11) D.S.Howse and W.Lucan: Sci.&Tech.of Weld.&Join., 2000, vol.5, pp189-193.
12) H.C.Ludwig, Weld.J., 1968, vol.47, pp234s-240s.
13) D.Fan, R.H.Zhang, Y.F.Gu and M.Ushio: Trans.JWRI., 2001, vol.30, pp35-40.
14) S.Sire and S.Marya: Proceedings of the 7th International Symposium, Kobe, Japan, 2001, pp.113-118.
15) S.Sire and S.Marya: Proceedings of the 7th International Symposium, Kobe, Japan, 2001, pp.107-112.
16) T.Ohji, A.Make, M.Tamura, H.Inoue and K.Nishiguchi: J of Japan Weld. Soc., 1990, vol.8, pp54-58.
17) M.Tanaka, T.Shimizu, H.Terasaki, M.Ushio, F.Koshi-ishi and C.L.Yang: Sci.&Tech.of Weld.&Join., 2000, vol.5, 397-402.
18) C.R.Heiple, J.R.Roper, R.T.Stagner and R.J.Aden: Weld.J., 1983, vol.62, pp72s-77s.
19) S.P.Lu, H.Fujii, H.Sugiyama, M.Tanaka and K.Nogi: Mater.Trans., 2002, vol.43, pp2926-2931.
20) S.P.Lu, H.Fujii, H.Sugiyama and K.Nogi: Metall.& Mater.Trans. 2003, vol.34A, pp1901-1907.
21) S.P.Lu, H.Fujii, H.Sugiyama, M.Tanaka and K.Nogi, ISIJ Int., 43 (2003) 1590-1595.
22) J.J.Lowke, M.Tanaka and M.Ushio, the 57th Annual Assembly of International Institute of Welding, Osaka, Japan, 2004, IIW Doc.212-1053-04.
23) S.P.Lu, H.Fujii and K.Nogi, Mater.Sci.&Eng.A, 2004, vol.380, pp290-297.
24) S.P.Lu, H.Fujii and K.Nogi, Scripta Mater., 2004, vol.51, pp271-277
25) K.C.Mills, B.J.Keene, R.F.Brooks and A.Shirali: Phil.Trans.R.Soc.Lond., 1988, vol.356A, pp911-925.
26) P.Sahoo.T.Debroy and M.J.Mcnallan: Metall.Trans., 1988, vol.19B, pp483-491.
27) K.Ishizaki, N.Araki and H.Murai: J. Jap. Weld. Soc., 1965, vol.34, pp146-153.
28) H.Taimatsu, K.Nogi and K.Ogino: J.High.Temp.Soc., 1992, vol.18, pp14-19.
29) P. Burgardt and C.R. Heiple: Weld J., (1986), vol.65, pp150s.-155s.
30) R.E. Sundell, H.D. Solomon, L.P. Harris, L.A. Wojcik, W.F. Savage and D.W. Walsh: Interim Report to the National Science Foundation, SRD-83-006, 1983, General Electric Co., Schenectady, N.Y.
31) A.A. Shirali and K.C. Mills: Weld J., 1993, vol.72, pp347s-353s.
32) S.P.Lu, H.Fujii and K.Nogi: ISIJ International, 2005, vol.45, lpp66-70.
33) N.S. Tsai and T.W. Eagar: Metall. Trans., 1985, vol.16B, pp841-846.
34) M.Tanaka, H.Terasaki, M.Ushio and J.J.Lowke: the 56th Annual Assembly of International Institute of Welding, Bucharest, Romania, 2003, IIW Doc.212-1040-03.